Relationship of Stopped Flow to Steady State Parameters in the Dimeric Copper Amine Oxidase from *Hansenula polymorpha* and the Role of Zinc in Inhibiting Activity at Alternate Copper-Containing Subunits†

Kenichi Takahashi‡ and Judith P. Klinman*

Department of Chemistry and Department of Molecular and Cell Biology, University of California, Berkeley, California 94720

Received October 26, 2005; Revised Manuscript Received February 9, 2006

ABSTRACT: The expression of a copper amine oxidase (CAO) from *Hansenula polymorpha* in *Saccharomyces cerevisiae* under differing culture conditions leads to the incorporation of varied levels of CAO-bound zinc. The presence of substantial amount of zinc results in two distinctive enzyme species, designated as the fast and slow enzymes. Both forms are rapidly reduced by substrate methylamine with a rate constant of 199 s^{-1} but behave remarkably differently in their oxidation rates; the fast enzyme is oxidized by dioxygen at a rate of 22.1 s^{-1}, whereas the slow enzyme reacts at a rate of 1.8×10^{-4} s^{-1}. The apparent k_{cat} of the enzyme preparation is linearly proportional to the fraction of the fast enzyme, with an extrapolated value of 6.17 s^{-1} when the enzyme is 100% in its "fast" form. A comparison of rate constants for cofactor reduction and reoxidation steps, measured in stopped flow experiments, to the extrapolated k_{cat} implicates additional steps in the steady state reaction. Measurement of the proportion of oxidized ($ETPQ_{ox}$) and reduced cofactor ($ETPQ_{red}$) under steady state conditions indicates approximately 50% of each cofactor form at 0.8 or 2 mM methylamine. Kinetic isotope effect measurements using deuterated amine substrate lead to the following steady state values: $^{D}(k_{red}) = 8.5$ (0.5), $^{D}(k_{cat}) = 1.7$ (0.1), and $^{D}(k_{cat}/K_m) = 4.3$ (0.2). The collective data allow the calculation of partially rate-determining constants during the reductive half-reaction (ca. 200 s^{-1} for binding of substrate to $ETPQ_{ox}$ and 27.9 s^{-1} for release of aldehyde product or a protein isomerization from $ETPQ_{red}$); an additional step with a rate constant of 13.2 s^{-1} is assigned to the oxidative half-reaction, most likely for the release of product hydrogen peroxide. These results, together with the sole detection of oxidized and reduced cofactor during rapid scanning stopped flow experiments, indicate that four steps contribute to k_{cat}, with the first electron transfer from cofactor to O_2 contributing ca. 29%. An investigation of the relationship between the copper content and the extent of the fast enzyme shows that only the copper-containing homodimer is capable of rapid reoxidation and that zinc−copper heterodimers are incapable of rapid turnover at either subunit. This implies communication between the metal sites of the two subunits per dimer that impacts O_2 binding and/or electron transfer from reduced cofactor to bound O_2.

The copper amine oxidases (CAOs,[1] EC 1.4.3.6) are distributed over a wide range of organisms, from bacteria and fungi to plants and animals. These enzymes catalyze the oxidative deamination of primary amines to form the corresponding aldehyde and ammonia, with subsequent reduction of dioxygen to hydrogen peroxide. This reaction enables microorganisms to utilize primary amines as a nitrogen source. The physiological significance of the CAOs in mammals is less clear, with emerging evidence for their role in inflammation in endothelial tissue and glucose uptake in the adipocyte. These enzymes are homodimers with each 75−80 kDa subunit containing two essential cofactors: a cupric ion and a unique organic cofactor, 2,4,5-trihydroxyphenylalanine quinone (topa quinone or TPQ), derived from a tyrosine protein side chain in a posttranslational modification process (*1*−*4*).

The role of TPQ in amine oxidation is summarized in Scheme 1. Basically, the CAO reaction is divided into two parts, reductive and oxidative half-reactions, proceeding via a ping-pong mechanism. In the reductive half-reaction, TPQ_{ox} reacts with the substrate amine to form the substrate Schiff base (SSB). The proton abstraction at C-1 of the substrate yields the product Schiff base (PSB), which is subsequently hydrolyzed to release the product aldehyde, leaving an aminoquinol form of TPQ (TPQ_{red}). Resonance Raman spectroscopy of TPQ_{ox} showed that the C−O moiety at C-5 has far greater double-bond character than that at C-2 or C-4 (*5*). This observation, together with the fact that the produc-

† This work was supported by grants from the National Institutes of Health (GM25765 and GM39296).

* To whom correspondence should be addressed. Telephone: (510) 642-2668. Fax: (510) 643-6232. E-mail: klinman@berkeley.edu.

‡ Present address: Department of Medical Biochemistry, Kurume University School of Medicine, 67 Asahi-machi, Kurume 830-0011, Japan. Telephone: 81-942-31-7544. Fax: 81-942-31-4377. E-mail: ktakahas@med.kurume-u.ac.jp.

[1] Abbreviations: AGAO, *Arthrobacter globiformis* phenylethylamine oxidase; BSAO, bovine serum amine oxidase; CAO, copper amine oxidase; HPAO, *H. polymorpha* amine oxidase; ICP, inductively coupled plasma; MeAm, methylamine; MeAm-d_3, trideuterated methylamine; topa, 2,4,5-trihydroxyphenylalanine; TPQ, topaquinone; TPQ_{ox}, oxidized form of TPQ; TPQ_{red}, reduced or aminoquinol form of TPQ; TPQ_{sq}, semiquinone form of TPQ; YNB, yeast nitrogen base.

10.1021/bi0521893 CCC: $33.50
Published on Web 03/21/2006

Scheme 1: Proposed Mechanism of the CAO Reaction[a]

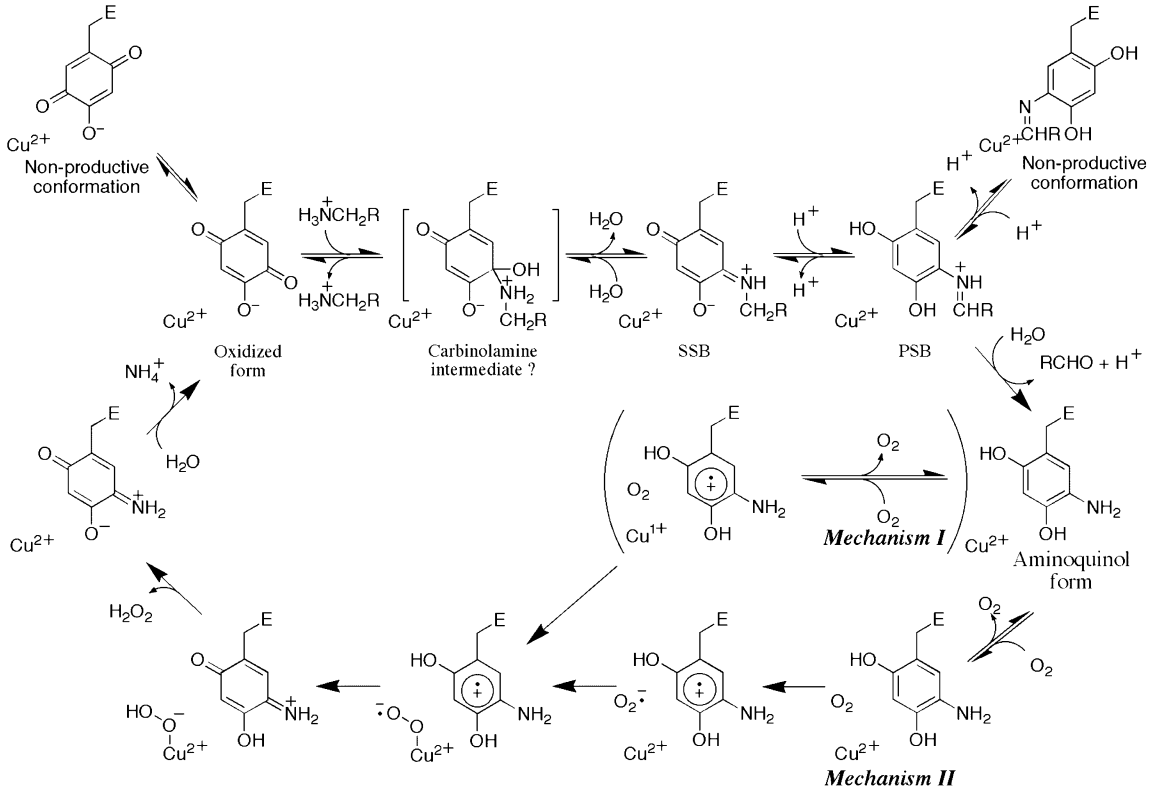

[a] SSB and PSB are substrate and product Schiff bases, respectively. In mechanism I, dioxygen binds to Cu^{1+} to form superoxide. In mechanism II, dioxygen binds at a non-metal site and is reduced directly by TPQ_{red}.

tive conformation of TPQ has the C-5 carbonyl oriented toward the substrate-binding site (*6*, *7*), explains the exclusive nucleophilic attack at the C-5 position by substrates and their analogues. Additionally, both the resting and reduced forms of TPQ have been shown to be unusually mobile, capable of occupying nonproductive conformations that involve a flipping of the cofactor ring, often in the direction of the active site copper (*1*, *2*).

In contrast to the well-established mechanism for the reductive half-reaction, there still remains uncertainty in the oxidative one, especially with regard to the function of the bound metal. Cofactor reoxidation indisputably includes the interaction of dioxygen with TPQ_{red} to produce hydrogen peroxide and iminoquinone; the iminoquinone intermediate either is hydrolyzed to release ammonia and to regenerate TPQ_{ox} or reacts directly with amine substrate to form the substrate Schiff base. Initially, copper was assumed to be essential for transferring electrons from TPQ_{red} to dioxygen. This was based, first, on the observation that TPQ_{sq} existed in the substrate-reduced form of selected CAOs under anaerobic conditions (*8*) and, second, on the observation that an electron could be transferred at a catalytically competent rate from TPQ_{red} to the cupric ion (*9*). In other words, a TPQ_{sq}/Cu^{+} species was proposed to bind and activate dioxygen as the first step in the oxidative half-reaction (mechanism I in parentheses in Scheme 1). Subsequently, detailed kinetic and metal substitution studies from this laboratory have led to an alternative mechanism for the copper amine oxidases from *Hansenula polymorpha* (HPAO) and from bovine serum. This involves initial dioxygen binding at a non-metal site, followed by electron transfer from TPQ_{red} to form the superoxide anion (mechanism II in Scheme 1) (*10*, *11*). According to the latter mechanism, the first one-electron reduction of dioxygen is the rate-determining step in the process of forming bound hydrogen peroxide from $ETPQ_{red}$ and O_2 (*11*) and contrasts with the former mechanism in which TPQ_{sq} may be expected to accumulate. In support of mechanism II, rigorous studies of the cobalt-substituted enzyme, which should not be capable of producing a TPQ_{sq}/Co^{1+} given the ca. 800 mV more negative redox potential for Co^{2+} than Cu^{2+} (*6*, *12*), have yielded high k_{cat} values (*13*). It has been proposed that the primary role of the metal is to provide electrostatic stabilization during a reduction of dioxygen to superoxide anion. Interestingly, the capacity of metals other than copper to activate the CAOs is highly dependent on the source of the enzyme, with studies of eukaryotic enzymes providing the primary support for mechanism II (*14*−*16*). The identification of a likely off-metal binding site for dioxygen in HPAO has provided additional support for the role of metal as an electrostatic stabilization catalyst (*7*, *17*).

In this study, we have turned to rapid kinetic analyses of the heterologously expressed wild-type eukaryotic CAO from *H. polymorpha* (HPAO) to confirm and investigate aspects revealed from prior steady state analyses. These studies confirm that the rate-determining step of the HPAO reaction sequence resides in the oxidative half-reaction, with the first one-electron reduction of dioxygen contributing ca. 29% to k_{cat}. As a result of subtle changes in growth conditions during enzyme expression, we were unexpectedly obligated to characterize an enzyme that contained varied proportions of copper and zinc. These studies reveal a dependence of k_{cat} on the fraction of protein that contains copper in *both* subunits of the dimer; i.e., enzyme containing zinc in one

of its subunits is inactive at the alternate subunit during the oxidative half-reaction. This apparent cooperativity, which is seen solely in the portion of the reaction that involves O_2, is discussed in the context of the structural properties of HPAO at its dimer interface.

MATERIALS AND METHODS

Chemicals and General Methods. All chemical materials were purchased from commercial providers and used without further purification except as noted. Glucose oxidase (*Aspergillus niger*) and catalase (bovine liver) were obtained from Sigma-Aldrich. Trideuterated methylamine (MeAm-d_3, 99% pure) was also purchased from Sigma. All argon used here was passed through a basic solution of pyrogallol to scrub oxygen. Buffers and protein solutions used in anaerobic experiments were degassed either by bubbling with argon or by stirring or applying gentle agitation under a stream of scrubbed argon. The oxygen concentration of buffers was measured using a Clark electrode. Data are represented as an average ± the standard error, based on, at least, three independent experiments.

Enzyme Expression and Purification. Wild-type HPAO was expressed in *Saccharomyces cerevisiae* and purified mainly according to the method described by Plastino et al. (*18*) with the slight modification of Mills and Klinman (*10*); *S. cerevisiae* was grown in the synthetic minimal medium containing 0.67% yeast nitrogen base (YNB) without amino acids, 0.5% ammonium sulfate (Sigma), and 2% glucose supplemented with 100 mg/L adenine, 100 mg/L histidine, 100 mg/L tryptophan, 150 mg/L leucine, and 5 μM $CuSO_4$.

In several cases, HPAO was expressed in a culture in which the concentration of YNB was decreased to 0.17% and that of $CuSO_4$ was increased to 10 μM, according to the original report about the synthetic minimum medium (*19*). Cultures (18 L) for each condition yielded approximately 120 and 70 mg of purified protein (more than 90% pure as judged on SDS−PAGE), respectively. Protein concentrations were determined by the Bradford assay (Bio-Rad).

General Characterization of HPAO. The quantitation of TPQ content was carried out by adding a 5-fold molar excess of a freshly prepared solution of phenylhydrazine HCl to an HPAO sample in the presence of 100 mM potassium phosphate buffer (pH 7.0). Spectra were recorded at 25 °C with a Hewlett-Packard 8452A diode-array spectrophotometer equipped with a thermostated cell holder until the increase in the absorbance at 448 nm due to TPQ-phenylhydrazone formation stopped (typically within 30 min). An extinction coefficient (*20*) of 40 500 M^{-1} cm^{-1} at 448 nm and a subunit molecular weight (*21*) of 75 700 were used to calculate the percentage of active TPQ cofactor in the protein. An extinction coefficient (*22*) of 1850 M^{-1} cm^{-1} at 480 nm was employed for TPQ_{ox}. In this study, concentrations of HPAO indicate the concentration of TPQ that is reactive to phenylhydrazine, unless otherwise noted.

The initial velocity of the HPAO reaction, including deuterium isotope effects, was measured by monitoring the rate of oxygen consumption using a Clark electrode. Reactions were performed in the presence of 100 mM potassium phosphate buffer (pH 7.0) and varied concentrations of MeAm and oxygen at 25 °C, as previously described (*11*). The ionic strength was adjusted to 300 mM with KCl. The data were fitted to the Michaelis−Menten equation by nonlinear regression using Kaleidagraph (Abelbeck Software).

Trace metal analyses were performed on a Perkin-Elmer 3000DV ICP-AES instrument using commercially available metal standard solutions. Samples were dialyzed overnight against an at least 200-fold excess volume of 100 mM potassium phosphate buffer (pH 7.0) prior to ICP analysis, as well as the rapid and steady state kinetic analyses. The metal content of the protein preparations was corrected for buffer contamination, which was normally close to background levels.

Rapid-Scanning Stopped Flow Spectrophotometry and Fast Kinetic Analysis. All aerobic and anaerobic stopped flow experiments were carried out at 25 °C in the presence of 100 mM potassium phosphate buffer (pH 7.0), with an ionic strength of 300 mM, on a Hi-Tech KinetAsyst SF-61 DX2 double-mixing stopped flow system equipped with a KinetaScan diode-array detector.

In a 5 mL gastight syringe which was sealed with a rubber septum at the top and connected to the drive syringe via a Luer-Lok fitting at the bottom, enzyme and substrate MeAm solutions were made anaerobic by degassing under reduced pressure for 5 min and passing argon with gentle agitation for 10 min. This manipulation was performed through the needles penetrating the rubber septum and was repeated three times. The solutions in the drive syringe were then allowed to temperature equilibrate for at least 5 min. For the measurement of the oxidative half-reaction, a double-mixing method was employed; 80 μM HPAO was first mixed with an equal volume (60 μL) of the same molar concentration of the methylamine solution. After an aging time of 50 s, half of the substrate-reduced enzyme was mixed with an equal volume (60 μL) of the same buffer containing twice the desired final concentration of oxygen, and the spectral change due to the oxidation of TPQ_{red} was recorded every 1.5 ms.

For the reductive half-reaction, glucose oxidase and catalase (50 units/mL each) were added to both the enzyme and substrate solutions, to achieve strict anaerobicity (*23*). After being made anaerobic in the manner stated above, a β-D-glucose solution, which had been degassed by bubbling scrubbed argon for at least 1 h while stirring, was added to a final concentration of 20 mM with the aid of a gastight microsyringe. Typically, a 25 μM HPAO solution was mixed with the same volume (120 μL) of substrate solution containing a varied concentration of methylamine in a single mixing method, and the spectral change due to TPQ reduction was recorded every 1.5 ms. Pseudo-first-order rate constants for reduction and oxidation of HPAO estimated from absorbance changes at 480 nm (the apparent k_{red} and k_{ox}, respectively) were calculated by nonlinear regression to a single-exponential equation using a program in Kinetasyst II (Hi-Tech) or Kaleidagraph (Abelbeck Software).

Alternatively, substrate-induced reduction of HPAO was observed at the saturated oxygen concentration. Both the enzyme (typically 15 μM) and the MeAm (0.8 or 2.0 mM) solutions were saturated under a stream of oxygen instead of argon (vide supra) with gentle agitation for 60 min. After equal volumes of each solution were mixed in a single-mixing device of the stopped flow, the change in spectra was recorded every 75 ms. In this experiment, it is expected

that, at an initial MeAm concentration (0.8 mM) that is lower than the oxygen level, a certain proportion of enzyme will be reduced by substrate and then reoxidized after the substrate is depleted. On the other hand, it is expected that, at an initial MeAm concentration (2.0 mM) that is greater than the oxygen level, all of the enzyme will ultimately be reduced after oxygen is depleted. As stated below, because the apparent oxidation rates of reduced HPAO are almost the same between ambient and saturated oxygen concentrations, the reaction mixture will be kept in the steady state until a substantial amount of oxygen is consumed. Therefore, this experiment enables us to investigate the ratio of the oxidized and reduced forms of HPAO in the steady state.

Spectroscopic Measurements of the HPAO Reaction. These were performed to investigate if all of the enzyme would be properly reoxidized and participate in the catalytic cycle or, alternatively, whether a substantial portion of enzyme would become inactivated during the catalytic turnover. All spectroscopic measurements of the HPAO reaction were carried out at 25 °C in the presence of 100 mM potassium phosphate buffer (pH 7.0), with an ionic strength of 300 mM, and spectra were recorded every 50 s.

An 0.85 mL sample of 7 μM HPAO was placed with stirring in a semi-micro quartz cuvette for the Hewlett-Packard 8452A diode-array spectrophotometer; after equilibration with atmospheric oxygen for 10 min, spectra were recorded. Four hundred seconds after the beginning of the spectral recording, 6.0 μL of 100 mM methylamine (final concentration of 0.7 mM, 100-equimolar) was added. After the substrate was depleted and the enzyme was reoxidized, another 50- or 100-equimolar methylamine was added. This cycle was repeated several times.

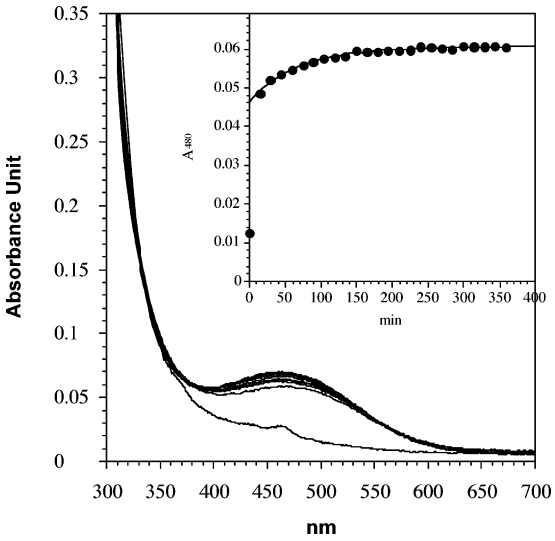

FIGURE 1: Spectral measurement of the oxidative half-reaction of substrate-reduced HPAO. Spectra were recorded every 15 min for 6 h. In a Carry 3 Bio UV−visible spectrophotometer (Varian), HPAO was degassed in a hand-crafted cuvette having a bulbous top and a ground glass joint under a stream of scrubbed argon through the needle penetrating the rubber septum for 60 min with stirring. After addition of 5-equimolar methylamine, which was made anaerobic in the same manner, with a gastight microsyringe through the other needle penetrating the septum, the first spectrum was immediately recorded. The solution was then oxygenated, by removing the septum, under the air stream during the interval of spectra for 60 min. The inset shows the time trace of the absorbance change at 480 nm. The line is a single-exponential fitting to the slow phase reoxidation. Conditions: 25 μM HPAO (entry 6 in Table 1), 125 μM methylamine, 100 mM KP_i, pH 7.0, and μ = 300 mM at 25 °C. The scan speed was 600 nm/min.

RESULTS

Heterogeneity of HPAO Expressed in S. cerevisiae. In our early preparations of HPAO that were expressed in a culture medium that contained the higher concentration of yeast nitrogen base (see Materials and Methods), it was found that the substrate-reduced HPAO was not fully reoxidized in a rapid phase. Typically, as shown in Figure 1, fully reduced enzyme was only partially reoxidized in the initial portion of the reaction, with completion of the reaction requiring several hours. As illustrated in the inset of Figure 1, the oxidation reflects two exponential processes characterized by rate constants that differ by 5 orders of magnitude: the fast enzyme with a k_{ox} of 22.1 s^{-1} (vide infra) and the slow enzyme with a k_{ox} of (1.8 ± 0.3) × 10^{-4} s^{-1}.

The extent of the fast and slow reactions appeared to fluctuate among protein preparations. The protocol in Figure 2 was designed to address the fraction of the fast reaction for each enzyme preparation. In these experiments, which contained 100 equimolar equivalents of MeAm, the diffusion of oxygen was too slow to replenish the oxygen instantaneously. Thus, the entire enzyme initially underwent complete reduction; i.e., the reaction system became nearly completely anaerobic, leading to the disappearance of TPQ_{ox} at 480 nm (Figure 2, bottom) or the appearance of TPQ_{red} at 310 nm (Figure 2, top). Subsequently, after the substrate was depleted, a certain portion of the enzyme was quickly reoxidized (fast enzyme), followed by the much slower oxidation (Figure 1, inset, and Figure 2). Importantly, the extent of the fast reaction did not change after the sequential additions of additional 50-equimolar aliquots of MeAm (Figure 2). Lee et al. (*24*) showed that a side species such as benzoxazole could be formed during the reaction of plasma amine oxidase with benzylamine in the presence of hydrogen peroxide and that the enzyme became partially inactivated under these conditions. The results illustrated in Figure 2 argue against the formation of an inactive or less active species during the catalytic turnover as the origin of a slow enzyme form. Indeed, there was no difference in the amounts of TPQ which were derivatized with phenylhydrazine for unreacted samples of enzyme in relation to those that had undergone full reoxidation after being treated with substrate (data not shown).

The extent of the fast enzyme for six preparations characterized in this study is summarized in Table 1, together with steady state kinetic parameters, the amount of TPQ, and copper and zinc contents. Although nickel and cobalt were also analyzed by ICP, those were within a background level. The amount of fast enzyme appeared to be correlated with metal content; this will be discussed later. As indicated in Figure 3, the fact that the apparent k_{cat} linearly correlated to the percent of fast enzyme not only demonstrated that the fast enzyme is solely responsible for the catalytic turnover but also made it possible to estimate the true k_{cat} value by extrapolating to 100% fast enzyme. This k_{cat} value of 6.17 ± 0.24 s^{-1} will be used as a reference in relating the fast kinetic analyses to steady state parameters. For the reaction of MeAm with HPAO (entry 5 in Table 1) at saturating oxygen concentrations, the noncompetitive deuterium isotope

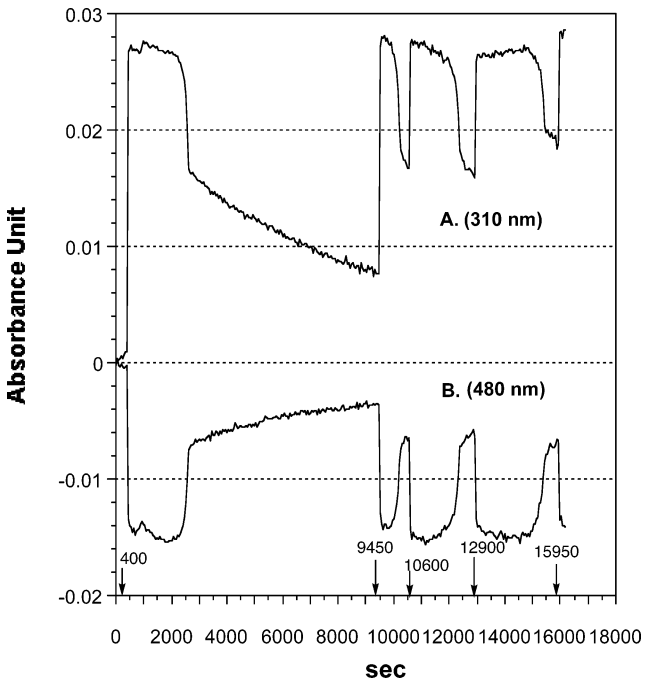

FIGURE 2: Spectroscopic measurements of the HPAO reaction. The time courses of absorbance changes at 310 (A) and 480 nm (B) accompanied with reduction and oxidation of TPQ are shown by using HPAO preparation 3 (Table 1). The reaction conditions are described in Materials and Methods. At 400, 9450, 10 600, 12 900, and 15 950 s, 100-, 50-, 50-, 75-, and 100-equimolar MeAm was added, respectively.

effects for k_{cat} and k_{cat}/K_m were 1.7 ± 0.1 and 4.3 ± 0.2, respectively (Table 2).

Fast Kinetic Analyses. Stopped flow kinetic experiments were carried out with substrate MeAm (0.67−37.5 mM) in excess over enzyme (12.5 μM) for the reductive half-reaction or with oxygen (10−520 μM) in the presence of 20 μM HPAO for the oxidative half-reaction. As stated above, many of our enzyme preparations exhibited heterogeneous reactivity (i.e., fast and slow reoxidation rates). To eliminate any ambiguity that might be caused by this heterogeneity, the data presented in this section were obtained by using HPAO (entry 5 in Table 1), the enzyme preparation consisting of 90% fast enzyme. We note that the data obtained with other preparations led to no significant difference in rate constants, which is reasonable because single-turnover kinetics are expected to yield constants that are independent of the concentration of the more active form of the enzyme. Additionally, the extent of enzyme reduction by MeAm under anaerobic conditions appeared to be independent of zinc content.

In Figure 4, apparent rate constants for the reduction of HPAO by substrate and the reoxidation of TPQ_{red} were plotted as a function of MeAm and oxygen concentrations, respectively. No characteristic spectral change other than a single-exponential decrease or increase of 480 nm, together with the concomitant increase or decrease of 310 nm signals, was observed in the reductive or oxidative half-reaction, respectively. Both the plots were fitted to the following equation:

$$k_{app} = k[S]/(K_S + [S]) \quad \text{(i)}$$

where k and k_{app} are the true and apparent rate constants, respectively, for the reduction of TPQ_{ox} by MeAm (k_{red}) and for the oxidation of TPQ_{red} (k_{ox}) by dioxygen, [S] is the concentration of substrate, MeAm, or dioxygen, and K_S stands for the apparent dissociation constant of HPAO with MeAm ($K_{S,MeAm}$) or dioxygen (K_{S,O_2}). The values thus obtained are summarized in Table 2. The deuterium isotope effect on k_{red} (8.5 ± 0.5) is slightly smaller than the ^Dk value of 9.6−13.5 reported for bovine plasma amine oxidase (BSAO) (*25*) but is likely to be close to the intrinsic isotope effect for cleavage of the C−H bond (*26*).

Ratio of Reduced and Oxidized HPAOs in the Steady State. According to the microscopic rate constants and steady state parameters obtained above, 199 s^{-1} for k_{red}, 22.1 s^{-1} for k_{ox}, and 6.17 s^{-1} for k_{cat}, at least one slower step (k_x) should exist in the overall HPAO reaction.

$$1/k_{cat} = 1/k_{red} + 1/k_{ox} + 1/k_x \quad \text{(ii)}$$

By using eq ii, k_x is calculated to be 8.9 s^{-1}. If the k_x step resides in the reductive half-reaction, the proportion of oxidized enzyme (E_{ox}) at steady state is calculated as follows:

$$E_{ox}/E_{total} = (1/k_{red} + 1/k_x)/(1/k_{red} + 1/k_{ox} + 1/k_x) \quad \text{(iii)}$$

Similarly, if the k_x step resides in the oxidative half-reaction, the proportion of reduced enzyme (E_{red}) at steady state is also calculated as follows:

$$E_{red}/E_{total} = (1/k_{ox} + 1/k_x)/(1/k_{red} + 1/k_{ox} + 1/k_x) \quad \text{(iv)}$$

In the former case, 72% of the total enzyme should be in the oxidized form, and in the latter case, 97% of the enzyme should be in the reduced form at steady state. Therefore, the investigation of the ratio of oxidized and reduced forms of HPAO at steady state is indispensable to assigning k_x to the reaction mechanism.

Fortunately, the apparent k_{ox} was almost the same when the oxygen concentration was elevated above the atmospheric concentration (Figure 4B). These data indicated that the HPAO reaction could be kept in the steady state until more than 80% of the dioxygen was consumed if the reaction was started at a saturating oxygen concentration and there was an adequate concentration of MeAm (more than 5-fold higher than K_{MeAm}) when the reaction system reached the atmospheric oxygen level.

Figure 5 shows the time trace of the absorbance change at 480 nm when the HPAO reaction was initiated at the saturating oxygen concentration in the presence of 0.8 or 2.0 mM MeAm. At 0.8 mM MeAm, the entire reaction could be divided into four phases. First, approximately half of HPAO was reduced by substrate quickly, and a short period of steady state turnover followed. As MeAm was consumed, the oxidation rate overcame the net reduction rate, and the apparent proportion of reduced enzyme began to decrease. Finally, MeAm was depleted, and all of the HPAO returned to its oxidized state (Figure 5, top trace). On the other hand, at 2.0 mM MeAm, there was a longer-lasting steady state, in which excess MeAm and oxygen remained following the initial reduction of enzyme; only when the oxygen was depleted did the enzyme undergo full reduction (Figure 5, bottom trace). The proportion of initially reduced HPAO was 49.0 ± 1.8 and 48.9 ± 2.1% after beginning with 0.8 and 2.0 mM MeAm, respectively. The integration of these findings with the steady state and single-turnover rate

Table 1: Summary of HPAO Preparations

HPAO	k_{cat} (s^{-1})	K_{MeAm} (mM)	K_{O_2} (μM)	TPQ (mol/subunit)	Cu^{2+} (mol/subunit)	Zn^{2+} (mol/subunit)	level of fast enzyme (%)
1[a]	2.16	0.15	28.8	0.49 (0.04)	0.74 (0.01)	0.52 (0.00)	40.2 (3.1)
2[a]	1.16	0.14	13.3	0.55 (0.03)	0.46 (0.01)	0.76 (0.00)	19.4 (2.5)
3[a]	2.96	0.28	10.6	0.52 (0.02)	0.79 (0.00)	0.48 (0.00)	46.8 (4.7)
4[a]	1.18	0.20	11.3	0.55 (0.03)	0.59 (0.00)	0.73 (0.01)	23.0 (3.1)
5[b]	5.82	0.23	nd[c]	0.51 (0.03)	1.20 (0.05)	0.06 (0.01)	89.4 (3.2)
6[b]	2.94	0.24	11.6	0.54 (0.05)	0.96 (0.01)	0.33 (0.00)	53.3 (1.1)
average		0.21 ± 0.04	15.1 ± 5.5				

[a] Expressed in the culture containing 0.67% YNB supplemented with 5 μM $CuSO_4$. [b] Expressed in the culture containing 0.17% YNB supplemented with 10 μM $CuSO_4$. [c] Not determined.

Table 2: Measured Constants and Isotope Effects for HPAO

parameter	average $\pm$ standard error
reduction rate constant (k_{red})[a]	199 ± 15 s^{-1}
oxidation rate constant (k_{ox})[a]	22.1 ± 1.1 s^{-1}
deuterium isotope effect for k_{red} ($^{D}k_{red}$)[b]	8.5 ± 0.5
apparent dissociation constant for MeAm ($K_{S,MeAm}$)[a]	8.8 ± 1.8 mM
apparent dissociation constant for oxygen ($K_{S,ox}$)[a]	15.4 ± 2.8 μM
deuterium isotope effects in the steady state[c]	
$^{D}[k_{cat}/K_m(amine)]$	4.3 ± 0.2
$^{D}(k_{cat})$	1.7 ± 0.1

[a] The conditions for these stopped flow experiments are described in Materials and Methods and Results sections. [b] This is the average obtained by dividing k_{red} values at protiated MeAm concentrations of 5.0, 12.5, and 37.5 mM with those for trideuterated MeAm at the same concentrations. [c] The conditions for the steady state experiments are described in Materials and Methods.

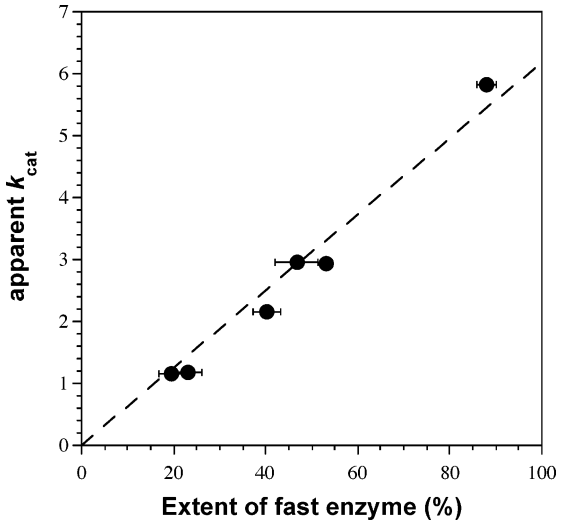

FIGURE 3: Relation between the apparent k_{cat} and the level of fast enzyme. The apparent k_{cat} value of each preparation was plotted as a function of the level of fast enzyme (see Table 1). The dashed line is a linear regression of the plot.

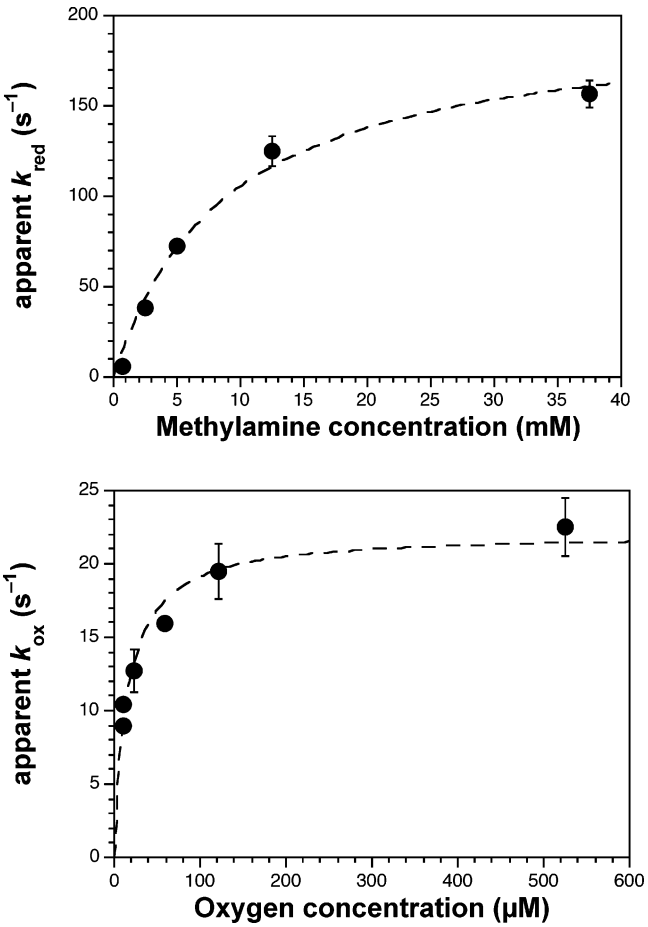

FIGURE 4: Effects of substrate MeAm and oxygen concentration on microscopic rate constants of HPAO reduction and reoxidation. (A) The final MeAm concentration was varied from 0.67 to 37.5 mM. (B) The final oxygen concentrations were varied from 10 to 520 μM. The lowest oxygen concentration (ca. 10 μM) was estimated by the total degree of HPAO oxidation. The dashed lines are theoretical fittings (see the text). The detailed reaction conditions are also described in the text.

constants requires a further separation of k_x into two steps: one of these involves the oxidized form of the enzyme ($k_x = 13.2$ s^{-1}) with the second occurring from the reduced enzyme ($k'_x = 27.9$ s^{-1}).

Relation between the Metal Content and the Extent of Fast Enzyme. As stated above, the proportion of the reduced enzyme that underwent rapid oxidation under stopped flow conditions was apparently correlated with the copper and zinc content of each enzyme preparation (Table 1). This is illustrated in Figure 6, where the extent of the fast reaction is seen to increase as a function of the moles of copper per subunit. This initially implied that the copper-containing subunits might be assigned to the fast enzyme and the zinc-containing subunits to the slow enzyme. However, *this predicts a linear relationship between the extent of the fast enzyme and the copper content, whereas the observed relationship is parabolic*.

It is well documented that each subunit of HPAO homodimer requires 1 mol of cupric ion for full activity (*6*). In our preparations, as seen in other experiments with HPAO (*10*), 1.2−1.3 metal ions per subunit was detected. At this moment, it is not clear why each subunit contains somewhat

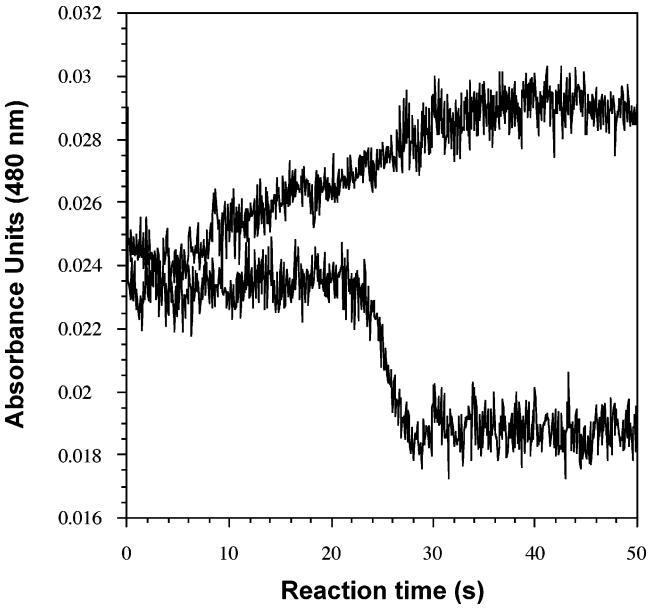

FIGURE 5: Time course of the HPAO reaction with MeAm at saturating oxygen concentrations. The time traces of the absorbance change at 480 nm in the presence of 0.8 (top) and 2.0 mM (bottom) MeAm are shown. Conditions: 7.5 μM HPAO type 5 (see Table 1), 100 mM KP_i, pH 7.0, μ = 300 mM, and 25 °C.

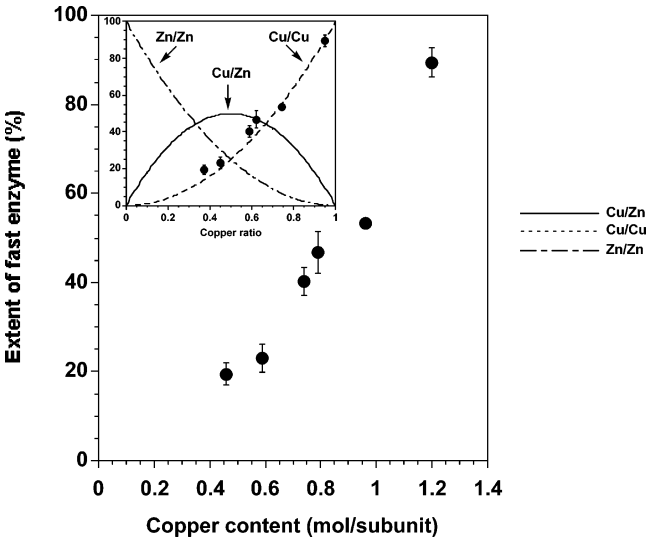

FIGURE 6: Relation between the level of fast enzyme and copper content. The level of fast enzyme was plotted as a function of copper content (see Table 1 for data). The inset shows the copper content was normalized as [Cu]/([Cu] + [Zn]). Lines are possible theoretical curves of the amounts of copper homodimer (dashed line), copper−zinc heterodimer (solid line), and zinc homodimer (dashed and dotted line); those were obtained by a simple binominal calculation, namely, $([Cu] + [Zn])^2 = [Cu]^2 + 2[Cu][Zn] + [Zn]^2$, where [Cu] + [Zn] = 1.

more than one metal ion, although evidence of ancillary metal sites is accumulating (cf. *27*−*29*). The parabolic correlation between the extent of the fast enzyme and the copper content becomes more obvious when the data are replotted as a function of the ratio of copper to the total amounts of metal per subunit (Figure 6, inset). The theoretical curves in the inset of Figure 6 represent the amount of copper homodimer (dashed line), copper−zinc dimer (solid line), and zinc homodimer (dashed and dotted line) and were based on the assumptions that metal content did not alter the affinity of the subunits for each other and that the binding of copper and zinc to the metal center of the catalytic site had occurred in a statistical manner. What became very clear from this kind of analysis was that the extent of the fast enzyme was correlated to the amount of copper-containing homodimer, implying a requirement for copper at both subunits for observation of full oxidative activity.

DISCUSSION

Presence of Zinc Ion as the Origin of Kinetic Heterogeneity in HPAO Expressed in S. cerevisiae. One remarkable feature of this study is that our preparations of HPAO contain two different enzyme species, a fast enzyme and a slow enzyme. Both are quickly reduced by MeAm but behave quite differently with respect to their reoxidation rates: 22.1 s^{-1} for the fast enzyme and 1.8×10^{-4} s^{-1} for the slow enzyme. The origin of a slowly reoxidizing form of the enzyme was initially considered in the context of either an "off the path", unprotonated product Schiff base, as seen in wild-type BSAO and the E406N mutant of HPAO (*5*, *30*), or a side reaction generating an inactive species such as benzoxazole (*24*). The latter was eliminated on the basis of the observation that repeated cycling between the reduced and oxidized enzyme did not alter the fraction of slow enzyme (see Results and Figure 2). Similarly, we consider it unlikely that a nonproductively bound PSB of TPQ is the origin of the slow enzyme observed in this study: (1) no accumulation of the diagnostic 380 nm species (*5*, *30*) was observed in catalytic turnover of the HPAO samples; (2) as noted above, no correlation was observed between the proportion of the slow enzyme form and the number of catalytic turnovers (Figure 2); and (3) reduction of HPAO by relatively large primary amines such as ethylamine and benzylamine, which have been reported to prevent the formation of the nonproductive conformation of the PSB (*30*), did not affect the extent of the slow enzyme reaction (data not shown). Thus, we conclude that the slow enzyme is not an inactive or less active side species formed during catalytic turnover but is present in the original protein preparation. One important property of the slow species is that it possesses the potential to be fully reoxidized (Figure 1) and to react with phenylhydrazine after complete oxidation (see Results).

As summarized in Table 1 and shown in Figure 6, the fraction of fast enzyme appears to correlate with the proportion of copper and zinc in each enzyme preparation. Namely, the presence of substantial amounts of zinc to generate heterodimeric HPAO is linked to the formation of the slow enzyme;[2] the mechanistic significance will be discussed below. In this section, we attempt to understand the origin of the elevated zinc content in many of the preparations described herein (Table 1). In relation to this question, Cai et al. reported that HPAO expressed in *S. cerevisiae* using culture medium that was supplemented with 0.17% YNB but lacking exogenously added copper contained more zinc than copper (*31*); the authors concluded that zinc was inserted into the heterologously expressed HPAO in the

[2] Alternatively, a referee has suggested that differences in protein folding or assembly may have been the source of variations in the metal content and the slow phase during the oxidative half-reaction. We consider this highly unlikely, given that the reductive half-reaction is essentially unaltered for all forms of the enzyme that were studied.

Scheme 2: Minimal Ping-Pong Mechanism for the HPAO Reaction[a]

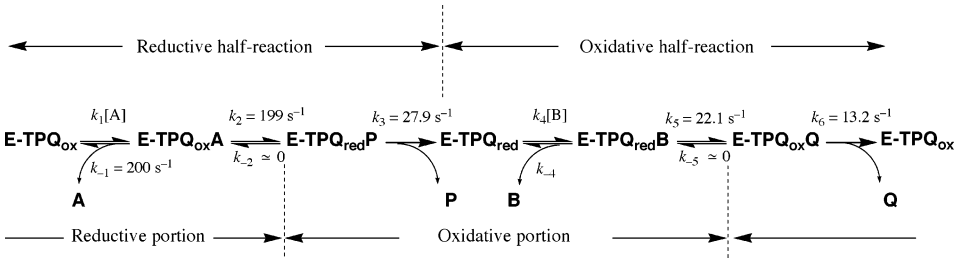

[a] A, B, and P stand for the first and second substrates, MeAm and dioxygen, and the first product, formaldehyde, respectively. Q represents the second products, ammonia and hydrogen peroxide.

absence of sufficient copper. In this study, the HPAO preparation composed of the highest fraction of the fast enzyme (ca. 90%, HPAO, entry 5 in Table 1) was obtained using culture medium containing 0.17% YNB supplemented with 10 μM cupric sulfate, showing that the final metal levels in HPAO depend on the composition of metal in the culture medium. Additionally, in the course of these studies, the concentration of YNB was changed in addition to that of added copper, with numerous preparations being obtained from media containing a 4-fold higher concentration of YNB (0.67%) supplemented with 5 μM cupric sulfate. As seen in Table 1, HPAO types 1−4 in Table 1 expressed under this condition contained elevated zinc levels, indicating that an increased level of YNB can achieve the same effect as reduced copper.

It is also true that we are unable to account quantitatively for the final levels of copper solely on the basis of the concentrations of metal and YNB in the media. In fact, HPAO type 6 in Table 1, which was expressed in the same culture medium as HPAO type 5 in Table 1, still contained 0.33 mol/subunit of zinc and a proportion of fast enzyme that was only 53%. In addition, the zinc contents of HPAO types 1−4 fluctuated from 0.48 to 0.76 mol/subunit despite having been prepared under the same culture condition. At present, we are unable to discern what additional factors are affecting the metal levels of HPAO samples expressed under the same culture condition, and studies to address this issue, e.g., variations among individual yeast cells, changes in growth curves, etc., lie outside the scope of this work.

Comparison of Pre-Steady State to Steady State Behavior Implicates Four Kinetic Processes Contributing to k_{cat}. The comparison of the rate constants for the reduction of TPQ by MeAm (199 s^{-1}) and the reoxidation of TPQ_{red} (22.1 s^{-1}) with the extrapolated k_{cat} value (6.17 s^{-1}) revealed that these two microscopic steps alone cannot determine the steady state turnover rate of HPAO, implicating at least one other step in the kinetic mechanism. Investigation of the proportion of oxidized and reduced forms in the steady state further implicated one additional step; as a result, four steps are concluded to contribute to the steady state turnover rate: k_{red}, k_{ox}, and k_x (13.2 s^{-1}) and k'_x (27.9 s^{-1}). Note that k_x pertains to a step that involves TPQ_{ox} and k'_x to TPQ_{red}, namely, the reductive and oxidative portions of the entire HPAO reaction consisting of k_6 up through k_2 and k_3 to k_5, respectively (see Scheme 2).

In attempting to identify the chemical species that correspond to k_x and k'_x, we find it is useful to first turn to the measured deuterium kinetic isotope effects on k_{cat}/K_m(MeAM) and k_{red} (Table 2) in the context of the ping-pong mechanism of Scheme 2. The portion of the reaction that corresponds to k_{cat}/K_m(MeAm) involves substrate binding up through the first irreversible step, which is likely to be the reduction of E−TPQ_{ox} to E−TPQ_{red} (see below). Given that k_x is from E−TPQ_{ox} and contributes to k_{cat}, it would have to reside between the E−TPQ_{ox}A species and the E−TPQ_{red}P species to be placed within the segment of the reaction that corresponds to the reduction of cofactor by bound substrate. However, since the value for k_x is more than 10-fold smaller than k_{red}, this would be expected to reduce $^D[k_{cat}/K_m$(MeAm)] to approximately unity in contrast to the observed isotope effect of 4.3 (Table 2). The observation that $^D[k_{cat}/K_m$(MeAm)] is lower than $^Dk_{red}$ (4.3 vs 8.5) is most logically attributed to a partially rate-limiting binding of substrate to enzyme, allowing us to estimate a value of ca. 200 s^{-1} for k_{-1}, from Scheme 2:

$$^D[k_{cat}/K_m(\text{MeAm})] = (^Dk_2 + C_f + {}^DK_{eq}C_r)/(1 + C_f + C_r) \quad \text{(v)}$$

where $C_f = k_2/k_{-1}$, $C_r = k_{-2}/k_3$, $^DK_{eq}$ is the equilibrium isotope effect on the hydrogen transfer from methylamine to E−TPQ_{ox}, and k_2 is assigned to k_{red} from the stopped flow. Since the stopped flow studies showed virtually complete reduction of E−TPQ_{ox} to E−TPQ_{red} under anaerobic conditions, we conclude that C_r is close to zero, providing an estimate of k_{-1} from k_{red} and the measured isotope effects.

In light of the preceding discussion and the fact that k_x refers to an intermediate existing somewhere within a reductive portion of the overall HPAO reaction (Scheme 2), we needed to look further downstream for the origin of the species that corresponds to this rate constant. It has been unclear whether the iminoquinone formed from cofactor reoxidation is hydrolyzed first or directly attacked by the free amine substrate, making it unclear whether the TPQ_{ox} or its imino complex contributes to the steady state. In the case presented here, the failure to detect any absorbance at the expected 340 nm band for an iminoquinone species strongly suggests that iminoquinone hydrolysis is fast and, further, that the contribution of k_x to k_{cat} is derived from a relatively slow loss of one or both products (hydrogen peroxide and ammonia) from the E−TPQ_{ox}Q species. Our inability to detect the 410 nm band anticipated for a Cu(II)−peroxy species would appear to rule out a rate-limiting loss of H_2O_2 from an inner sphere copper complex; however, prior protonation to produce a protein-bound H_2O_2 is anticipated, and the loss of the resulting protein-bound H_2O_2 could be partially rate limiting. With regard to a slow loss of ammonia, this might be expected to produce a 340−350

nm band, arising from the impact of bound ammonia on the conformation of the active site cofactor (*18*); however, the ammonia released during the oxidative portion of the steady state oxidative half-reaction may reside in a site different from that seen when ammonia is added exogenously, preserving the 480 nm absorbance arising from TPQ_{ox}. We therefore propose that k_x corresponds to the loss of one or both products from the $E-TPQ_{ox}Q$ species (or, possibly, a conformational change that is necessary to "reset" the enzyme for its reaction with substrate amine). In previous steady state studies of the oxidative half-reaction of BSAO and HPAO, measured under conditions that reflected the binding of O_2 to the $E-TPQ_{red}$ species up through the first irreversible step, kinetic ^{18}O isotope effects led to identification of the first electron transfer from the reduced cofactor to O_2 as rate limiting. From this study, the two steps that control the complete oxidative half of the HPAO reaction are assigned to the initial electron transfer step (22 s^{-1}) and the release of one or both products (13 s^{-1}), contributing 37 and 63%, respectively, to the steady state portion of the reaction that occurs between $E-TPQ_{red}$ and free $E-TPQ_{ox}$ species (Scheme 2).

The results herein contrast with studies by Hirota et al. (*32*) who reported that intermediates with λ_{max}s at 310 and 340 nm appeared in the first 20 ms after mixing of the substrate-reduced AGAO with oxygen (*32*); these species were proposed to be a deprotonated and a protonated form of the iminoquinone, respectively. Since the decay of these intermediates was comparable to the increase in the 480 nm absorption, they postulated that the hydrolysis of TPQ iminoquinone to oxidized TPQ would be the rate-determining step in the oxidative half-reaction of AGAO. Despite very significant conservation of structure at the active sites of the members of the CAO family, a growing body of data implicates differences in rate-limiting steps for these enzymes.

With regard to the nature of k'_x (calculated to be 27.9 s^{-1}), this arises from an oxidative portion of the overall HPAO reaction (Scheme 2) and occurs prior to the introduction of O_2 (note that the reoxidation of the $E-TPQ_{red}$ species by O_2 as measured in the stopped flow is a single-exponential process with a rate constant of 22 s^{-1}). This leads to the assignment of k'_x to either the hydrolysis of the product Schiff base via a carbinolamine intermediate, the release of product formaldehyde, or a protein conformational change that is required to prepare the reduced enzyme for its subsequent reaction with O_2. The absence of the 380 nm species ascribed to the accumulation of the product Schiff base (*33*) further narrows the possibilities to either the loss of product formaldehyde or a protein conformational change. Note that the rapid mixing experiments that were conducted to measure k_{red} and k_{ox} would not detect this species, even though it lies between $E-TPQ_{red}$ and $E-TPQ_{ox}$ species. This is because of the nature of the stopped flow experiments, in which the species that was formed following enzyme reduction remained in the reaction chamber long enough, prior to the introduction of O_2, for the process that corresponds to k'_x to be complete.

To summarize, the comparison of the steady state turnover rate for HPAO to rate constants determined in the stopped flow, when coupled with the determination of the extent of oxidized and reduced enzyme forms that accumulate during the steady state, has led to the determination of four rate constants in the kinetic mechanism, k_{red}, k_{ox}, k_x, and k'_x that are assigned as shown in Scheme 2. Given the magnitude of k_{ox} for the electron transfer between the reduced cofactor and O_2, we conclude that electron transfer contributes 29% to the turnover rate under conditions of saturation of both substrate amine and O_2. Additionally, the comparison of steady state isotope effects to that in the presteady state allowed an estimation of k_{-1}, also shown in Scheme 2.

There are two further issues that we pursue below. We question, first, whether the measured deuterium isotope effect from stopped flow experiments is an intrinsic value [note that it is reduced from the value of ca. 13.5 measured with BSAO (*25*)] and, second, whether the K_S measured in the stopped flow can be construed as an approximate K_d for methylamine. One way to assess the latter is to use the values of the measured steady state isotope effects and K_m to estimate K_d (*25*):

$$({}^{D}k_{cat} - 1)/[{}^{D}k_{cat}/K_m(\text{MeAm}) - 1] = K_m/K_d \quad \text{(vi)}$$

This predicts a K_d value of 0.99 mM, a value 9-fold smaller than the measured value of K_s of 8.8 mM (Table 2). The weakest link in the calculation of eq vi is ${}^{D}k_{cat}$, due to the small size of this value. If we use a ${}^{D}k_{cat}$ value of 1.2 previously measured (ref *34* and discussion below), we calculate a value for K_d of 3.3 mM, much closer to, but still reduced from, the experimental value of 8.8 ± 1.8 obtained from the stopped flow. It is likely that the rate for substrate binding contributes to the observed transients for the reaction of the oxidized enzyme with methylamine at concentrations below saturation, elevating the measured $K_{s,MeAm}$ above K_d. In fact, this is anticipated from the values for k_{-1} and k_2 in Scheme 2, which predict a K_s ($=k_{-1} + k_2/k_1$) that is twice the true K_d.

In the same vein, we question whether the four rate constants shown in Scheme 2 can reproduce the measured isotope effect on k_{cat} of 1.7. Using the expression for ${}^{D}(k_{cat})$, eq vii allows us to assess this issue:

$${}^{D}(k_{cat}) = ({}^{D}k_2 + C_{vf} + {}^{D}K_{eq}C_r)/(1 + C_{vf} + C_r) \quad \text{(vii)}$$

where ${}^{D}k_2$ is assigned to ${}^{D}k_{red}$, ${}^{D}K_{eq}$ is the equilibrium isotope effect for substrate oxidation, $C_r = k_{-2}/k_3$, and $C_{vf} = k_2/k_3 + k_2/k_5 + (1 + k_{-5}/k_5)k_2/k_6$. As noted above, k_{-2} is expected to be close to zero. Similarly, the initial electron transfer from cofactor to O_2 is expected to be followed by rapid, downhill steps making $k_{-5} \sim 0$. We, thus, calculate a value of 1.2 for ${}^{D}(k_{cat})$, which is comparable to the previously reported one (*34*), using measured values for k_2 and k_5 and calculated values for k'_x (k_3) and for k_x (k_6). As noted above, a ${}^{D}(k_{cat})$ of 1.2 also provides the anticipated relationship between the calculated K_d for methylamine binding and the value of K_s estimated from the stopped flow. Overall, the aggregate data indicate that ${}^{D}k_{cat}$ is close to unity and that C−H abstraction is not significantly rate determining at saturating concentrations of both substrate and O_2 saturation. Further, all analyses support the conclusion that ${}^{D}k_{red}$ provides an excellent approximation of the intrinsic isotope effect on C−H bond cleavage.

Possible Cooperation between Subunits in the Oxidative Half-Reaction. It is well established that CAOs are functional

homodimers (*4*, *6*); this has been accompanied by considerable discussion regarding the possibility of communication between the subunits **(***6*, *7*, *27*, *28*, *34*). In particular, with regard to bovine serum amine oxidase, evidence has been presented alternately for half-of-the-sites reactivity during cofactor derivatization with hydrazine reagents (*35*) versus full reactivity for amine substrates during the reductive half-reaction of the catalytic cycle (*36*). From the studies of the eukaryotic HPAO presented herein, it is clear that cofactor reduction by methylamine takes place via a single-exponential process that appears independent of the presence of either copper or zinc ion at the metal binding site. In contrast, the parabolic correlation between the copper content of HPAO and the level of the fast enzyme (Figure 6) points to the conclusion that only a copper-containing homodimer is capable of rapid turnover, i.e., of generating the fast enzyme form. We note that our interpretation of the correlation between copper content and kinetic competence of the oxidative half-reaction is linked to the reasonable assumption of statistical binding of copper and zinc to the available metal sites, together with the less expected property that the copper content is uncorrelated with the presence of TPQ (see below); as a corollary, the data imply that subunit affinity is unaffected by the nature of the bound metal at each site.

In our preparations of HPAO, ~50% of the subunits possess TPQ independent of the copper and zinc levels (Table 1), a level of TPQ in the range typically observed for HPAO prepared by heterologous expression in *S. cerevisiae*. We note that this estimate of TPQ content, which is based on phenylhydrazine reactivity and a previously published extinction coefficient for the phenylhydrazine adduct, is slightly lower than the value estimated by absorbance at 480 nm for the underivatized cofactor; importantly, the estimated level of TPQ varies little from one preparation to another. Thus, while the level of the active enzyme correlates with the proportion of copper bound at both subunits, the level of TPQ does not. It is now well established that copper is the natural metal giving rise to TPQ formation and that zinc is inert in this process (*37*); further, once zinc ion is bound to the active site, it has not been possible to effect its replacement by copper, at least in vitro (*31*). If the TPQ in the protein preparations that have been characterized in this study were present solely in copper-containing subunits, i.e., once copper-bound and generated TPQ it could not exchange, we would expect our enzyme preparations to contain three kinds of subunits: copper-bound subunits with and without TPQ (TPQ−Cu and Tyr−Cu, respectively) and a zinc-bound subunit without TPQ (Tyr−Zn). This would impact the distribution of copper-containing subunits in the following way, for an illustrative enzyme preparation containing 0.6 mol of copper and 0.4 mol of zinc per mole of subunit with a TPQ content of 50%: 50% TPQ−Cu, 10% Tyr−Cu, and 40% Tyr−Zn. A simple trinominal evaluation of this protein preparation gives the proportion of possible dimers as follows: 25% TPQ−Cu/TPQ−Cu, 10% TPQ−Cu/Tyr−Cu, 40% TPQ−Cu/Tyr−Zn, 1% Tyr−Cu/Tyr−Cu, 8% Tyr−Cu/Tyr−Zn, and 16% Tyr−Zn/Tyr−Zn.[3] Because only TPQ-containing enzyme is measurable, and all our experiments have been normalized by the TPQ concentration, the dimerized enzymes responsible for the oxidation and reduction of TPQ would contribute in the following proportions: 50% TPQ−Cu/TPQ−Cu, 10% TPQ−Cu/Tyr−Cu, 40% TPQ−Cu/Tyr−Zn, where the percentage is shown as a ratio of TPQ content of each dimer to the total amount of TPQ. Application of this type of analysis to each of the enzyme preparations in Table 1 fails to give the observed correlation between copper content and activity shown in Figure 6. Indeed, the parabolic correlation between the copper content of HPAO and the level of the fast enzyme (Figure 6) could not be rationalized by any explanation until we accepted the supposition that zinc and copper were distributed among the enzyme subunits in an equal probability regardless of the presence of TPQ. Since no significant metal exchange is observed to occur in the purified HPAO (*31*), this proposal implicates significant mobility for the protein-bound metals in vivo as compared to their in vitro behavior. Upon reflection, this becomes plausible, as the cytoplasm of the *S. cerevisiae* cells in which HPAO was produced is far more reducing than the buffers used for enzyme purification and manipulation; it is well established that reductants facilitate the removal of copper from HPAO in its reduced, Cu^+ form (*38*, *39*). Additionally, the cytoplasm of the *S. cerevisiae* may be expected to contain many different molecules (including amines) with metal chelating activities and potential access to the HPAO active site.[4] In possible support of our model of metal exchange occurring after cofactor production during expression of HPAO in *S. cerevisiae*, the TPQ content of HPAO type 2 in Table 1 can be seen to slightly exceed the copper level. To our knowledge, no precedent is available that deals with the relation between metal type and TPQ content in CAOs, and only one of our preparations exhibits this feature. This issue would benefit from future study, in particular, with an experimental approach that permits correlating the amount of copper and TPQ, versus copper and Tyr, at each subunit.

We note that the results reported herein are unlikely to impact previous steady state kinetic studies that addressed the nature of the oxygen binding pocket in HPAO and the primary role of the reduced cofactor in outer sphere electron transfer to the bound O_2 (*10*, *11*, *13*). The consequence of the introduction of a very slow step (1.8×10^{-4} s^{-1}) for the reoxidation of reduced enzyme that is a hybrid of zinc and copper-containing protein is to reduce the concentration of enzyme that operates during steady state turnover; this is equivalent to adding less enzyme to the assay mixture. With regard to ^{18}O isotope effects that were obtained over time periods longer than those used in steady state assays, the fact that experimentally determined values for HPAO were constant over the entire time course (*11*, *13*) rules out possible artifacts from the participation of a very slow enzyme form with different properties.

[3] These are estimated as follows: $(0.5\text{TPQ}-\text{Cu} + 0.1\text{Tyr}-\text{Cu} + 0.4\text{Tyr}-\text{Zn})^2 = 0.25(\text{TPQ}-\text{Cu})^2 + 0.01(\text{Tyr}-\text{Cu})^2 + 0.16(\text{Tyr}-\text{Zn})^2 + 0.1(\text{TPQ}-\text{Cu})(\text{Tyr}-\text{Cu}) + 0.08(\text{Tyr}-\text{Cu})(\text{Tyr}-\text{Zn}) + 0.4(\text{Tyr}-\text{Zn})(\text{TPQ}-\text{Cu})$.

[4] One plausible, though unproven, model for the observed properties of the isolated HPAO would involve a fairly rapid addition of copper to the precursor, Tyr-containing protein to generate active enzyme in vivo. Subsequent exposure of the TPQ-containing enzyme to cytosol that contains a mixture of zinc and copper ions would then lead to the mixed metal populations isolated in this study. We expect that once Zn^{2+} is inserted into mature protein it is immobile, due to the fact that it is the reduced, Cu^+ form of the native metal that has been demonstrated to undergo metal removal and exchange in vitro.

The possible structural origin of cooperativity in the oxidative half-reaction of HPAO can be considered in the context of the dimer interface of the CAOs. As indicated from X-ray crystal structures, this region of the protein contains an extensively hydrated channel, with some water molecules forming a hydrogen-bonded network (*7*). The substrate O_2 is believed to enter its active site via this channel (*7*). Structural studies of binding of Xe to four members of the CAO class further implicate an O_2 binding region between the dimer interface and the final O_2 binding pocket (*40*). Significantly in the context of this discussion, the two TPQs and the two copper atoms per dimer are separated by 42.5 Å (Cα−Cα) and 34.6 Å, respectively (*7*), such that the two metal ions are unable to interact directly with each other. Examination of the HPAO structure, however, reveals an interesting and potentially important structural feature in which Asp630 and Arg646 are present on a long arm at the dimer interface, with Asp630 hydrogen bonding to His624 which serves as one of the ligands to the active site metal ion. Most interestingly, Asp630 from one subunit A enters into an interaction with Arg646 on the opposite subunit B. This network forms a possible origin of the observed cooperative effects reported herein. We suggest, as a working hypothesis, that the presence of zinc at subunit A may lead to an altered inner sphere geometry, which propagates to the metal's second sphere, disrupting the fine balance between Asp630 and Arg646 on opposing subunits. This may disrupt the copper at subunit B in such a way that it is no longer capable of supporting the rapid catalysis of reduction of O_2 to hydrogen peroxide. As a second possibility, the altered network from zinc at subunit A to copper at subunit B may perturb the pathway for O_2 binding or the O_2 pocket itself. While these ideas are only speculative for the moment, they offer a framework for future experimental testing. Previously, the CAOs have been shown to be highly unique enzymes, with their active site copper ion performing dual roles involving, first, the facilitation of cofactor biogenesis and, second, the reduction of O_2 to hydrogen peroxide during catalytic turnover. The studies described herein suggest yet a third role for copper, that of maintaining a network of interactions at the dimer interface which is essential for efficient oxidative chemistry at either subunit.

ACKNOWLEDGMENT

We are grateful to Dr. Diana Wertz for providing us the recombinant yeast cell expressing wild-type HPAO. Dr. Nicole Samuels and Dr. John P. Evans are acknowledged for assistance in ICP analysis.

REFERENCES

1. Dove, J. E., and Klinman, J. P. (2001) Trihydroxyphenylalanine quinone (TPQ) from copper amine oxidases and lysyl tyrosylquinone (LTQ) from lysyl oxidase, in *Advances in Protein Chemistry* (Dove, J., and Klinman, J. P., Eds.) Vol. 58, pp 141−174, Academic Press, San Diego.
2. Dooley, D. M. (1999) Structure and biogenesis of topaquinone and related cofactors, *J. Biol. Inorg. Chem. 4*, 1−11.
3. Klinman, J. P. (2003) The multi-functional topaquinone copper amine oxidase, *Biochim. Biophys. Acta 1647*, 131−137.
4. Klinman, J. P. (1996) Mechanisms whereby mononuclear copper proteins functionalize organic substrates, *Chem. Rev. 96*, 2541−2561.
5. Nakamura, N., Moënne-Loccoz, P., Tanizawa, K., Mure, M., Suzuki, S., Klinman, J. P., and Sanders-Loehr, J. (1997) Topaquinone-dependent amine oxidases: Identification of reaction intermediates by Raman spectroscopy, *Biochemistry 36*, 11479−11486.
6. Mure, M., Mills, S. A., and Klinman, J. P. (2002) Catalytic mechanism of the topaquinone-containing copper amine oxidase, *Biochemistry 41*, 9269−9278.
7. Li, R., Klinman, J. P., and Mathews, F. S. (1998) Crystal structure of copper amine oxidase from *Hansenula polymorpha* determined at 2.4 Å resolution, *Structure 6*, 293−307.
8. Dooley, D. M., McGuirl, M. A., Brown, D. E., Turowski, P. N., McIntire, W. S., and Knowles, P. F. (1991) A Cu(I)-semiquinone state in substrate-reduced amine oxidase, *Nature 349*, 262−264.
9. Turowski, P. N., McGuirl, M. A., and Dooley, D. M. (1993) Intramolecular electron-transfer rate between active site copper and topaquinone in pea seedling amine oxidase, *J. Biol. Chem. 268*, 17680−17682.
10. Mills, S. A., and Klinman, J. P. (2000) Evidence against reduction of Cu^{2+} to Cu^{+} during dioxygen activation in a copper amine oxidase from yeast, *J. Am. Chem. Soc. 122*, 9897−9904.
11. Su, Q., and Klinman, J. P. (1998) Probing the mechanism of proton coupled electron transfer to dioxygen: The oxidative half-reaction of bovine serum amine oxidase, *Biochemistry 37*, 12513−12525.
12. Drummond, J. T., and Matthews, R. G. (1994) Nitrous oxide degradation by cobalamin-dependent methionine synthase: Characterization of the reactants and products in the inactivation reaction, *Biochemistry 33*, 3732−3741.
13. Mills, S. A., Goto, Y., Su, Q., Plastino, J., and Klinman, J. P. (2002) Mechanistic comparison of the cobalt-substituted and wild-type copper amine oxidase from *Hansenula polymorpha*, *Biochemistry 41*, 10577−10584.
14. Suzuki, S., Sakurai, T., Nakahara, A., Manabe, T., and Okuyama, T. (1983) Effect of metal substitution on the chromophore of bovine serum amine oxidase, *Biochemistry 22*, 1630−1635.
15. Agostinelli, E., De Matteis, G., Mondovi, B., and Morpurgo, L. (1998) Reconstitution of Cu^{2+}-depleted bovine serum amine oxidase with Co^{2+}, *Biochem. J. 330*, 383−387.
16. Padiglia, A., Medda, R., Pedersen, J. Z., Finazzi-Argo, A., Lorrai, A., Murgia, B., and Floris, G. (1999) Effect of metal substitution in copper amine oxidase from lentil seedlings, *J. Biol. Inorg. Chem. 4*, 608−613.
17. Goto, Y., and Klinman, J. P. (2002) Binding of dioxygen to non-metal sites in protein: Exploration of the importance of binding site size versus hydrophobicity in the copper amine oxidase from *Hansenula polymorpha*, *Biochemistry 41*, 13637−13643.
18. Plastino, J., Green, E. L., Sanders-Loehr, J., and Klinman, J. P. (1999) An unexpected role for the active site base in cofactor orientation and flexibility in the copper amine oxidase from *Hansenula polymorpha*, *Biochemistry 38*, 8204−8216.
19. Sherman, F. (1991) Guide to yeast genetics and molecular biology, in *Methods in Enzymology* (Guthrie, C., and Fink, G. R., Eds.) Vol. 194, pp 3−21, Elsevier, Amsterdam.
20. Cai, D., and Klinman, J. P. (1994) Copper amine oxidase: Heterologous expression, purification and characterization of an active enzyme in *Saccharomyces cerevisiae*, *Biochemistry 33*, 7647−7653.
21. Cai, D., and Klinman, J. P. (1994) Evidence for a self-catalytic mechanism of 2,4,5-trihydroxyphenylalanine quinone biogenesis in yeast copper amine oxidase, *J. Biol. Chem. 269*, 32039−32042.
22. Mure, M., and Klinman, J. P. (1995) Model studies of topaquinone, in *Methods in Enzymology* (Klinman, J. P., Ed.) Vol. 258, pp 39−52, Academic Press, San Diego.
23. Hartmann, C., Brzovic, P., and Klinman, J. P. (1993) Spectroscopic detection of chemical intermediates in the reaction of *para*-substituted benzylamines with bovine serum amine oxidase, *Biochemistry 32*, 2234−2241.
24. Lee, Y., Shepard, E., Smith, J., Dooley, D. M., and Sayre, L. M. (2001) Catalytic turnover of substrate benzylamines by the quinone-dependent plasma amine oxidase leads to H_2O_2-dependent inactivation: Evidence for generation of a cofactor-derived benzoxazole, *Biochemistry 40*, 822−829.
25. Palcic, M. M., and Klinman, J. P. (1983) Isotopic probes yield microscopic constants: Separation of binding energy from catalytic efficiency in the bovine plasma amine oxidase reaction, *Biochemistry 22*, 5957−5966.
26. Bell, R. P. (1973) in *The Proton in Chemistry*, 2nd ed., pp 250−296, Cornel University Press, Ithaca, NY.
27. Parsons, M. R., Convey, M. A., Wilmot, C. M., Yadav, K. D. S., Blakeley, V., Corner, A. S., Phillips, S. E. V., McPherson, M. J.,

and Knowles, P. F. (1995) Crystal structure of a quinoenzyme: Copper amine oxidase of *Escherichia coli* at 2 Å resolution, *Structure 3*, 1171−1184.
28. Wilce, M. C. J., Dooley, D. M., Freeman, H. C., Guss, J. M., Hatsunami, H., McIntire, W. S., Ruggiero, C. E., Tanizawa, K., and Yamaguchi, H. (1997) Crystal structure of the copper-containing amine oxidase from *Arthrobacter globiformis* in the holo- and apo- forms: Implications for the biogenesis of topaquinone, *Biochemistry 36*, 16116−16133.
29. Kumar, V., Dooley, D. M., Freeman, H. C., Mitchell Guss, J., Harvey, I., McGuirl, M. A., Wilce, M. C. J., and Zubak, V. M. (1996) Crystal structure of a eukaryotic (pea seedling) copper-containing amine oxidase at 2.2 Å resolution, *Structure 4*, 943−955.
30. Cai, D., Dove, J., Nakamura, N., Sanders-Loehr, J., and Klinman, J. P. (1997) Mechanism-based inactivation of a yeast methylamine oxidase mutant: Implications for the functional role of the consensus sequence surrounding topaquinone, *Biochemistry 36*, 11472−11478.
31. Cai, D., Williams, N. K., and Klinman, J. P. (1997) Effects of metal on 2,4,5-trihydroxyphenylalanine (topa) quinone biogenesis in the *Hansenula polymorpha* copper amine oxidase, *J. Biol. Chem. 272*, 19277−19281.
32. Hirota, S., Iwamoto, T., Kishishita, S., Okajima, T., Yamauchi, O., and Tanizawa, K. (2001) Spectroscopic observation of intermediates formed during the oxidative half-reaction of copper/topaquinone-containing phenylethylamine oxidase, *Biochemistry 40*, 15789−15796.
33. Mure, M., and Klinman, J. P. (1995) Model studies of topaquinone-dependent amine oxidases. II. Characterization of reaction intermediates and mechanism, *J. Am. Chem. Soc. 117*, 8707−8718.
34. Hevel, J. M., Mills, S. A., and Klinman, J. P. (1999) Mutation of a strictly conserved, active-site residue alters substrate specificity and cofactor biogenesis in a copper amine oxidase, *Biochemistry 38*, 3683−3693.
35. De Baise, D., Agostinelli, E., De Matteis, G., Mondovì, B., and Morpurgo, L. (1996) Half-of-the-sites reactivity of bovine serum amine oxidase: Reactivity and chemical identity of the second site, *Eur. J. Biochem. 237*, 93−99.
36. Janes, S. M., and Klinman, J. P. (1991) An investigation of bovine serum amine oxidase active site stoichiometry: Evidence for an aminotransferase mechanism involving two carbonyl cofactors per enzyme dimer, *Biochemistry 30*, 4599−4605.
37. Chen, Z., Schwartz, B., Williams, N. K., Li, R., Klinman, J. P., and Mathews, F. S. (2000) Crystal structure at 2.5 Å resolution of zinc-substituted copper amine oxidase of *Hansenula polymorpha* expressed in *Escherichia coli*, *Biochemistry 39*, 9709−9717.
38. Kishishita, S., Okajima, T., Kim, M., Yamaguchi, H., Hirota, S., Suzuki, S., Kuroda, S., Tanizawa, K., and Mure, M. (2003) Role of copper ion in bacterial copper amine oxidase: Spectroscopic and crystallographic studies of metal-substituted enzymes, *J. Am. Chem. Soc. 125*, 1041−1055.
39. Agostinelli, E., De Matteis, G., Sinibaldi, A., Mondovì, B., and Morprugo, L. (1997) Reactions of the oxidized organic cofactor in copper-depleted bovine serum amine oxidase, *Biochem. J. 324*, 497−501.
40. Duff, A. P., Trambaiolo, D. M., Cohen, A. E., Ellis, P. J., Juda, G. A., Shepard, E. M., Langley, D. B., Dooley, D. M., Freeman, H. C., and Guss, J. M. (2004) Using xenon as a probe for dioxygen-binding sites in copper amine oxidases, *J. Mol. Biol. 344*, 599−607.

BI0521893